

FABRICATION OF HIGHLY DENSE PURE 6H-SiC CERAMICS VIA THE PVT METHOD USING SUB-MICRON SiC POWDERS

#BOBO LIU, JIANFENG YANG

State Key Laboratory for Mechanical Behavior of Materials, Xi'an Jiaotong University,
Xi'an 710049, PR China

#E-mail: yupiner2003@163.com

Submitted July 4, 2019; accepted November 19, 2019

Keywords: Sub-micron SiC, Dense ceramics, Polycrystalline phase, PVT method

The dense SiC ceramics were prepared by the physical vapour transport (PVT) method using three types of SiC powder with different grain size, including a kind of SiC powder with a mean diameter of 500 nm. The effects of the grain size of the raw materials on the bulk density, bending strength and hardness of the SiC ceramics were studied. It was found that with a decreasing grain size, the bulk density and the bending strength of the fabricated SiC ceramics increased, while the Vickers hardness decreased. The effects of the grain size of the raw materials on the nucleation density and the growth rate of the SiC were analysed, and the growth characteristic of the SiC ceramics was systematically explored. The results indicated that the crystal type, the nucleation density and the growth rate were obviously affected by the soaking temperature. When the temperature was higher or lower than 2200 °C, the fabricated ceramics was composed of a 6H-SiC polycrystalline or the mixture of a 6H-SiC and 3C-SiC polycrystalline. Meanwhile, with an increasing temperature, the nucleation density decreased and the growth rate increased. Obviously, by optimising the fabrication process, highly dense 6H-SiC ceramics with a bulk density of 3.07 g·cm⁻³ and a bending strength of 335.6 ± 10 MPa could be rapidly fabricated by the PVT method using the sub-micron SiC powder.

INTRODUCTION

Dense silicon carbide (SiC) ceramics have been one of the most widely used high-performance structural components, owing to their high temperature strength, corrosion resistance, good thermal conductivity, oxidation resistance, and relatively low thermal expansion coefficient [1, 2]. However, its large-scale industrial application was always hindered due to the lack of high-performance density SiC ceramics [3-6]. Recently, a range of synthesis methods (such as the reaction sintering method, the hot-pressing sintering process, and the liquid-phase sintering technique) were reported for the fabrication of dense SiC ceramics by the sintering of SiC powders with the help of functional additives [8-9]. These traditional methods have the advantages of colder sintering temperatures (~1400 °C), high yield and low cost, and can be applied in an industrial production setting. Unfortunately, the remnants (sintering additives) might remain in the final products, which has a “weak” secondary phase, seriously degrading the excellent properties of the high-density SiC ceramics.

Additionally, it is very difficult to obtain high-density SiC ceramics without sintering additives, due to the covalent nature of the Si-C bonding and the low self-diffusion coefficient [15, 16]. Lately, Dai's group reported a novel physical vapour deposition (PVT) method for

the preparation of pure SiC ceramics. However, many problems remain to be solved. In the previous work, high-purity and high-density SiC ceramics were successfully fabricated by the PVT method [17]. The growth rate and the orientation of the SiC ceramics, the effects of the growth time and temperature on the grain size were explored.

However, the SiC ceramics only exhibited a bending strength of 290 ± 34 MPa because of the larger grain size (an average grain size of 2 mm). According to the fine grain strengthening mechanism, by decreasing the grain size it might be a potential way to increase the bending strength of the high-density SiC. On the basis of the theories of crystal growth, the primary reason for being responsible for the large crystal size was the low super-saturation which is beneficial to form the low-density nucleus of the SiC. On the contrary, large super-saturation in the growth chamber of high-density SiC facilitates the formation of a high-density nucleus which is good for obtaining the smaller grain size SiC by restricting the lateral growth of each nucleus. The latest research in the literature demonstrated that the smaller grain size of the raw materials could increase the super-saturation in the growth chamber. Therefore, in this study, with the aim of increasing the mechanical property of the high-density SiC ceramics, nano SiC powders (500 nm) were used as the raw material to fabricate high-density SiC by PVT,

and the effects of the nano SiC powder on the growth of SiC ceramics have been studied. It was found that the nucleation habits of high-density SiC have been refined, and its bending strength increased with the grain size of the raw materials decreasing as well.

EXPERIMENTAL

Raw materials

Commercial SiC powders of 175 μm (purity, 99.90 %; specific surface area, too small to test; Zaozhuang Liyuan SiC Co. Ltd., Zaozhuang, China), 50 μm (purity, 99.90 %; specific surface area, 0.018 $\text{m}^2\cdot\text{g}^{-1}$; Zaozhuang Liyuan SiC Co. Ltd., Zaozhuang, China) and 500 nm SiC powders (purity, 99.81 %, specific surface area, 20.012 $\text{m}^2\cdot\text{g}^{-1}$, Shanghai ST-nano science and technology Co. Ltd., China) were used as the raw materials, which were homogeneously mixed. The particle size of the different raw materials was measured by a Laser Particle Size analyser (Winner3003). Figure 1 shows that three particle size distributions of the raw material measurements, the particle size of the sub-micron materials has a probability distribution average at 500 nm. The same quality of the three types of silicon carbide raw materials were placed into the same graphite crucible at 2200 $^{\circ}\text{C}$ for 30 min. The results utilisation is shown in Table 1, it is the ratio of the graphite deposition on the substrate and the original weight. It can be seen that the utilisation increased with a decrease in the size of the raw materials, the utilisation of the sub-micron powders is 0.387 maximum. With the same sintering temperature, because of the large specific surface area of the sub-micron powder, the saturation vapour pressure, rapid evaporation rate and large growth rate can be seen. In the action, it is more economical to choose the sub-micron silicon carbide as the raw material.

Fabrication process

The density of the 6H-SiC SiC ceramics was prepared by the physical vapour transport (PVT) method at different temperatures (1900 $^{\circ}\text{C}$, 2000 $^{\circ}\text{C}$, 2100 $^{\circ}\text{C}$, 2200 $^{\circ}\text{C}$, 2300 $^{\circ}\text{C}$) using 175 μm , 50 μm and 500 nm SiC powders as the raw materials, respectively. The effects of the temperature and holding time on the grain size, growth rate, thickness and orientation of the silicon carbide were explored, and the concentration gradient, the random nuclei of the SiC on the polycrystalline phase

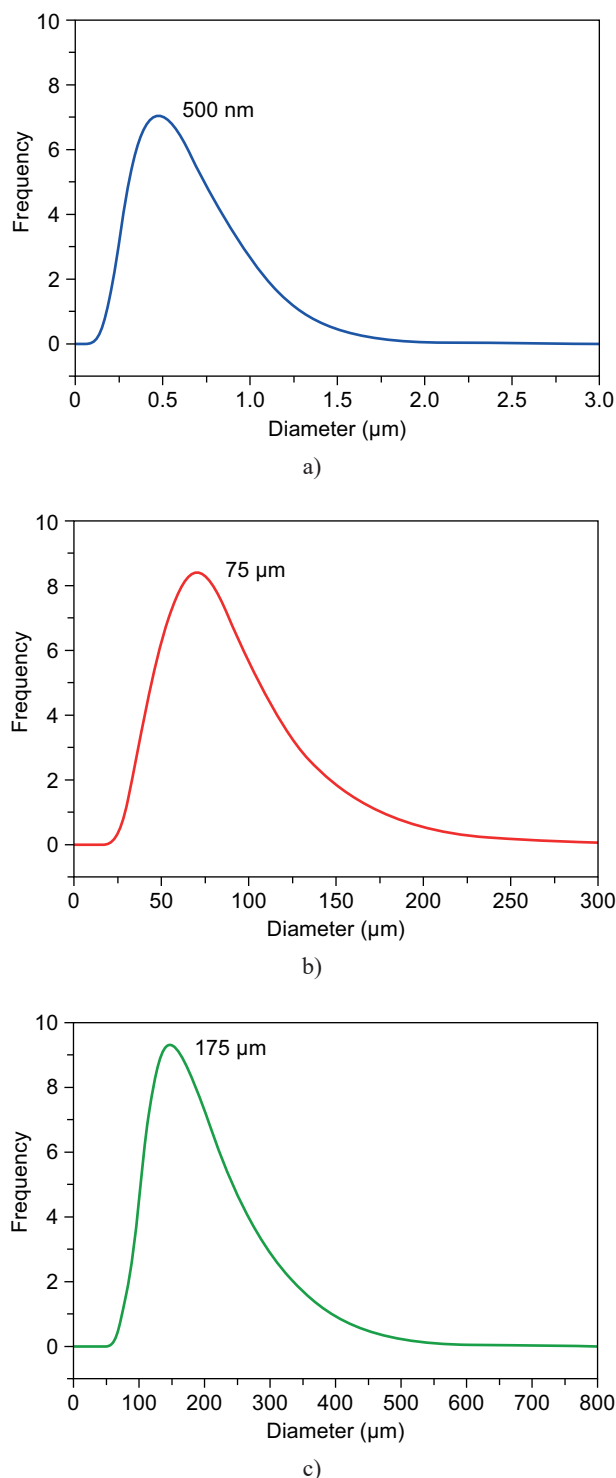


Figure 1. The measurements of the three particle size distribution of the raw powders.

Table 1. The results of the utilisation.

	Raw weight (g)	Residual (g)	Deposition on lid (g)	Loss (g)	Utilisation (%)
500 nm	3	0.85	1.16	0.99	38.7
75 μm	3	1.80	1.09	0.11	36.3
175 μm	3	1.03	1.01	0.96	33.7

growth during the SiC PVT growth were studied. The growth process consisted of the following steps: At first, the furnace was heated to 1273 K and held for 10 min at a pressure of about 10^{-3} Pa to volatilise the contaminated gas species. Then, argon with a pressure of 50 kPa was charged into the furnace and then the temperature was gradually increased to the growth temperature. The temperature of the bottom of the crucible was increased to 2200 ± 10 °C. Finally, the temperature at the bottom of the crucible was kept at the growth temperature and the system pressure of the argon gas was kept at 5×10^4 Pa. After growth, the polycrystalline SiC specimen with 100 mm in diameter and 8 mm in thickness could be prepared, and green SiCw could be obtained in the heat radiation holes of the upper carbon fibre felt.

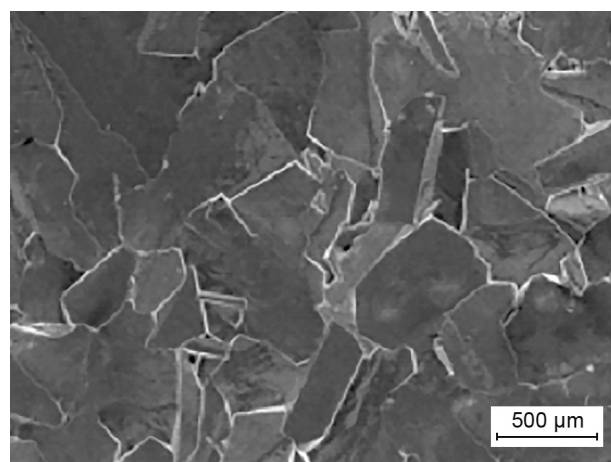
Characterisation techniques

The phase formation of the specimens was analysed by X-ray diffraction using Cu K α radiation. The microstructure was observed using a scanning electron microscopy system (JEOL JSM-6460). The average grain size was estimated by the Image-Pro Plus quantitative image analysis software (Version 7.0, Media Cybernetics, USA). The densities of the specimens were determined by the Archimedes method. The bending strengths of the specimens were tested via a three-point bending test (Model WDT-10) with a support distance of 20 mm, a crosshead speed of 0.5 mm min $^{-1}$ and the test including three samples, respectively. The Vickers hardness was tested with a load of 9.8 N using the OmniMet 88-7000 fully automated micro-indentation.

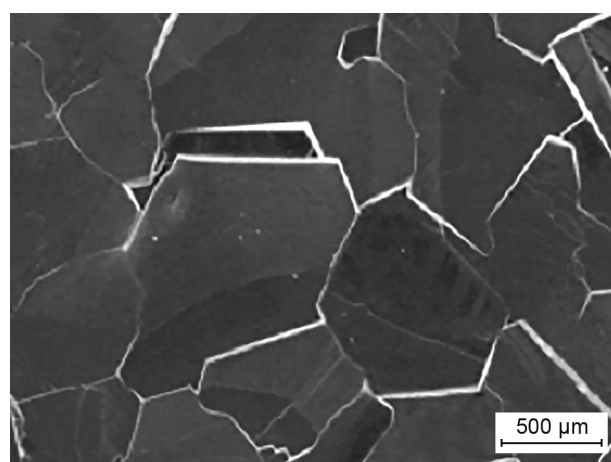
RESULTS AND DISCUSSION

The effects of the grain size of the raw materials on the mechanical properties of the SiC ceramics

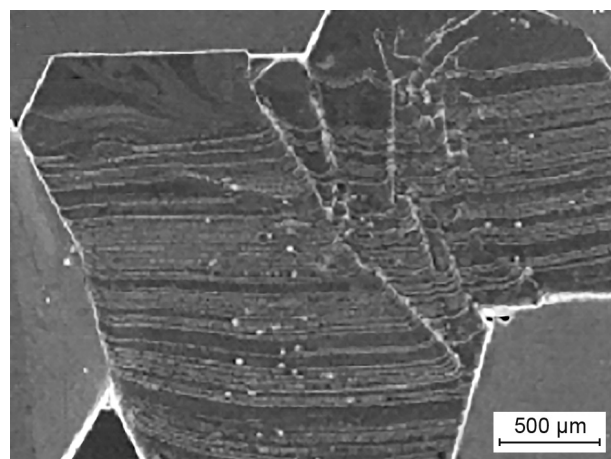
The mechanical properties of the SiC ceramics are listed in Table 2. The specimens exhibited very high bulk density and hardness. The bulk density of the sample using the 500 nm powders is 3.197 g·cm $^{-3}$, which is very close to the theoretical density of the SiC (3.211 g·cm $^{-3}$) and much higher than the density of the samples using 50 μ m and 175 μ m. While the bending strength is about 335.6 MPa, which is higher than the bending strength of using the 50 μ m and 175 μ m SiC powders. It is well known that the bending strength of the ceramic materials



a) 500 nm



b) 50 μ m



c) 175 μ m

Figure 2. The SEM of the sample using the different size powders for growing 2 h: a) 500 nm; b) 50 μ m; c) 175 μ m.

Table 2. The mechanical properties of the samples prepared at 2200 °C for 120 min.

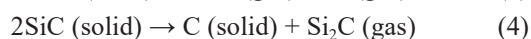
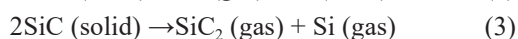
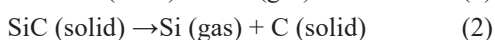
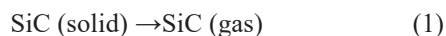
Size	Bending (MPa)	Vickers hardness (GPa)	Density (g·cm $^{-3}$)
175 μ m	290.0 \pm 7	29.7 \pm 0.04	3.10 \pm 0.005
50 μ m	311.1 \pm 5	28.9 \pm 0.08	3.08 \pm 0.006
500 nm	335.6 \pm 5	28.5 \pm 0.08	3.07 \pm 0.005

depends largely on the grain size and it decreased with an increase in the grain size, as explained by Carniglia using the Hall–Petch-type relationship [18-19]. In this study, the SiC grain size is mainly the reason which causes the low bending strength. Therefore, reducing the grain size is an important issue for improving the strength of the polycrystalline ceramics, and this will be investigated in the future. However, the Vickers hardness of the sample using 500 nm is lower than the samples using the 50 and 175 μm SiC powders. The reason for the lower Vickers hardness is that the size of the indentation is 100 μm (as shown in Figure 2), the basic grain size of the sample using 175 μm is greater than 500 μm , the indentation on the crack in the same grain; and the grain size of samples using 500 nm are less than 100 μm , with the grain boundary crack expanded, the indentation is very easy to extend.

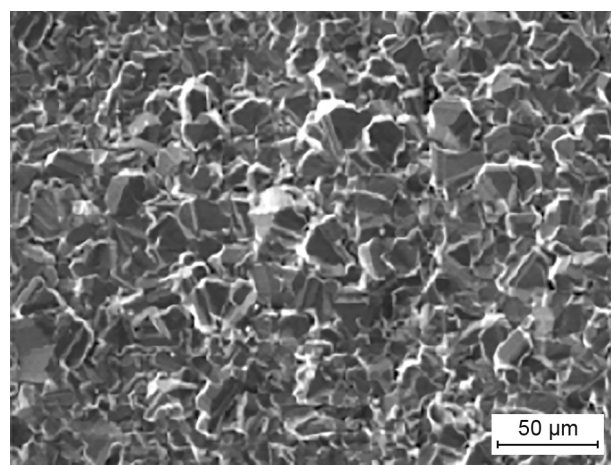
The effects of the grain size on
the nucleation density and growth
rate of the SiC ceramics

Figure 3 shows the grain size of the SiC nuclei using the different raw materials for 2 min at 2200 °C. It can be seen that the grain formed by the sub-micron powders is more uniform and smaller than that prepared by the other two raw materials. At the same time, the grain distribution of the sub-micron powders is more compact than that formed by the other two materials. However, the nucleation of the powder with the 75 μm and 175 μm particle sizes is dispersed and relatively larger, and the nucleation number is relatively smaller than that using the sub-micron powders as the raw material. The average grain size of the prepared material by using the sub-micron powders as the raw material is $33.13 \pm 0.008 \mu\text{m}$ (Figure 3a), and the average grain size of the prepared material by using the other two raw materials is $40.79 \pm 0.006 \mu\text{m}$ (Figure 3b) and $58.43 \pm 0.005 \mu\text{m}$ (Figure 3c), respectively. Because the sub-micron powders size is smaller, the surface area of the particles is larger, so the growth rate is faster than that prepared by the other two raw materials. Therefore, the compensates are the difference between the particle sizes of the raw materials, so that the grain size of the corresponding raw materials is so large, and the contact between the growth grains will be closer.

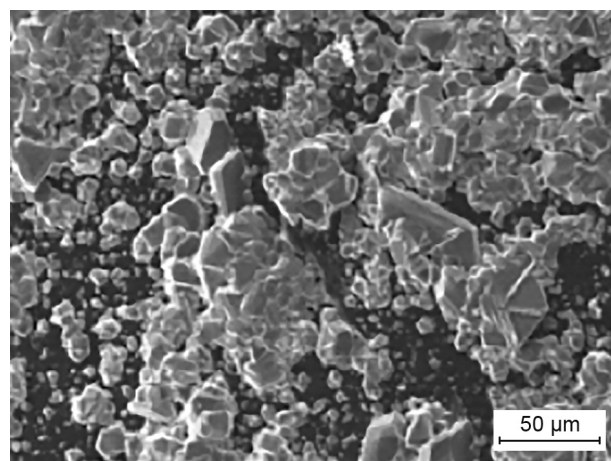
The principal stages during the PVT process were investigated based on the dissociative sublimation of the source material, the mass transport of the Si and C species to the substrate, and the deposition by condensation. The solid SiC was decomposed and could be interpreted by the following reactions:



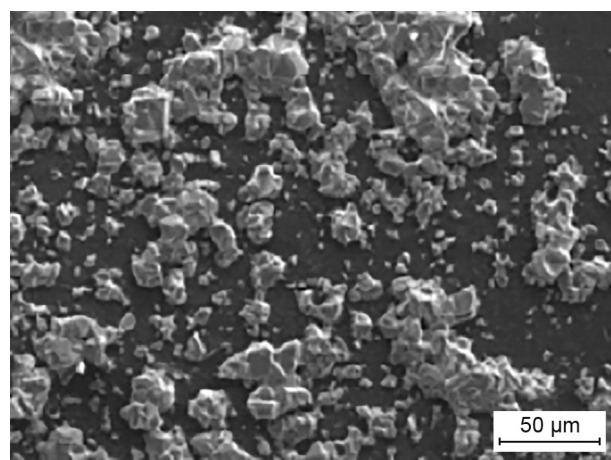
When the Si (gas) and SiC₂ (gas) diffuses to the edge of the substrate, it was easy to react with the carbon atoms on the graphite crucible lid and forms the SiC nuclei. Equations 1 ~ 4 are the sublimation and decomposition reactions of the SiC powders in the crucible at the high temperature. The predominant species



a) 500 nm



b) 50 μm



c) 175 μm

Figure 3. The SEM of the grain using the different size powders for growing 2 min: a) 500 nm; b) 50 μm ; c) 175 μm .

in the sublimated vapour were: Si, SiC₂ and Si₂C [20]. The equilibrium partial pressures of Si, Si₂C and SiC₂ were calculated at the different temperatures using [21]:

$$\log p_{\text{Si}} = 12.74 - 2.66 \times \frac{10^4}{T} \quad (5)$$

$$\log p_{\text{Si}_2\text{C}} = 15.10 - 3.62 \times \frac{10^4}{T} \quad (6)$$

$$\log p_{\text{SiC}_2} = 15.98 - 3.53 \times \frac{10^4}{T} \quad (7)$$

Figure 4 displays equilibrium vapour pressure of the gas phases (Si, SiC₂ and Si₂C) between 1950 °C and 2350 °C. It can be seen that the pressure of three gases increased when the temperature increased, while the Si partial pressure increases at 1900 - 2200 °C, and decreases above 2200 °C. the gas mixture of the Si-C in the Ar system, the mass transport was mostly driven by the temperature gradients, which lead to a difference in the vapour pressure between the source and the substrate [22]. The supersaturation of the vapour species is the driving force for the deposition of the vapour species at the growth front. The reaction between the Si or Si₂C atoms in the vapour phase with the carbon atoms on the graphite crucible lid forms the SiC nuclei. The condensation and deposition of the Si partial pressure on the SiC in the crucible facilitates the growth of the SiC grains.

In addition, the relationship between the equilibrium vapour pressure and the grain size could be expressed as:

$$\ln \frac{P}{P_0} = \frac{2M\gamma}{RTd} \quad (8)$$

where P refers to the equilibrium vapour pressure of the source material with a diameter of d , P_0 is the bulk material equilibrium vapour pressure, M is the material mole mass, and γ is the surface energy and R is the gas constant. According to Equation 8, when the grain size of the source material decreases, the equilibrium vapour

pressure would increase. Correspondingly, the difference in the partial vapour pressure among the vapour species would increase exponentially, which not only increases the absolute amount of the C component but also increases the Si-C ratio. It may be responsible for the larger decreasing ratio of the sublimation rates and the higher recrystallisation rates for the smaller grain size of the source material. The calculated results proved that the grain size of the source material could affect the effective heat-transfer coefficient of the source material, the supersaturation, and the ratio of the Si:C in the growth process of the SiC bulk single crystal by the PVT. Therefore, optimising the grain size of source material is an effective and convenient way to grow high-quality SiC bulk material in our experiment [23].

Figure 5 shows the grain size of SiC nuclei using the different raw materials at the different temperatures. The result shows the grain size of the SiC nuclei increased with the growth temperature lower than 2200 °C, and decreased with the growth temperature higher than 2200 °C. While the grain size of the SiC nuclei increased with the increased size of the raw material, the grain size of the used sub-micron powder is more uniform than using the other raw material and has an average size between 11 µm ~ 40 µm. However, the grain size of 50 µm grade powder is between the 13 µm ~ 80 µm range larger and causes scattered nucleation, the grain size of the 175 µm grade powder is in the range of 43 µm ~ 110 µm. It is also reported that the proper temperature and the raw material were two key factors in the SiC growth region, the temperature guaranteed the evaporation of the raw materials to form the catalyst and promoted the nucleation and growth of 6H-SiC, while the raw vapour obtained by the heat radiation holes in the carbon fibre felt facilitated the transportation and transition of the vapour specials [19]. In addition, it can also be found in the figure that the size of the grain size is associated with the particle size of the raw materials at the same temperature.

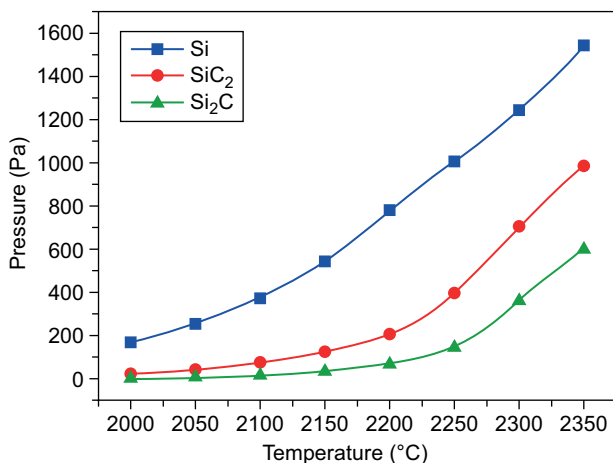


Figure 4. The equilibrium vapour pressure of the gas phase (Si, SiC₂ and Si₂C) between 1950 °C and 2350 °C.

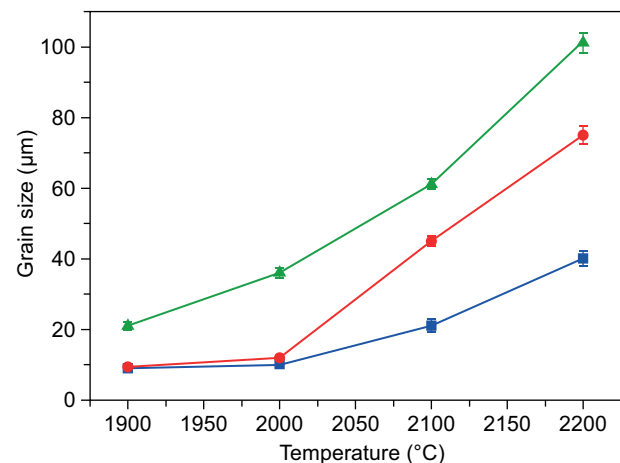


Figure 5. The grain size of the SiC nuclei using the different raw materials at the different temperature.

Figure 6 shows the growth rate of the SiC using the different raw materials for 30 min at the different temperatures, where the growth rate is the ratio of the thickness and the growth time by preparing a thick sheet to be measured, reducing the raw material silicon carbide. At different temperatures, the growth rate of the same powders was firstly increased and then decreased when the growth temperature was above 2200 °C. This phenomenon is different from the report by Dai [17], where they found the growth rate increases with the increasing temperature and temperature gradient. They thought the main factors influencing the growth rate of the SiC ceramics were the temperature and the temperature gradient. But in our experiment, there no temperature gradient exists, the vapour transmission path in the powders may play an important role in the growth process, as when the temperature increases the Si atoms on the substrate surface reacts to the evaporation, the Si

atoms over the substrate surface vapour and the pressure decreases, so the growth rate gradually decreases. The growth rate of the 500 nm powder was the quickest. With the increasing temperature from 2100 °C to 2250 °C, the maximum value of the growth rate using the 500 nm powder was $0.17 \text{ mm} \cdot \text{min}^{-1}$ at 2200 °C, this is larger than using the 50 μm and 175 μm powder, whose maximum value is $0.075 \text{ mm} \cdot \text{min}^{-1}$ and $0.075 \text{ mm} \cdot \text{min}^{-1}$, respectively. On the other hand, it is difficult to exactly test the density of the sample obtained at a time less than 30 min. In the initial stage, the crystal growth is mainly in nucleation, the bulk SiC materials were difficult to obtain for short times. On the other hand, the purpose of this paper is to investigate the densification process of the polycrystalline SiC by the PVT method, the sample is not compact when the time is less than 30 min, and the main work is focused on the nucleation process emphatically at the period.

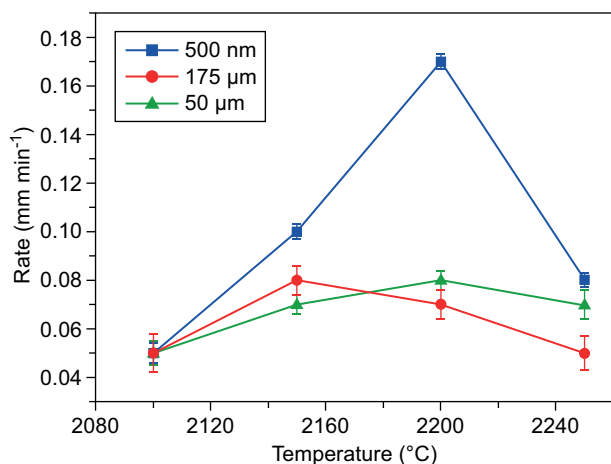


Figure 6. The growth rate of the SiC at the different sintering temperatures using the different raw materials.

The effects of the sintering temperature on the crystal type and growth morphology of the SiC ceramic using the 500 nm powder

Figure 7 shows that the XRD patterns of the SiC ceramic grows 60 min at the different sintering temperature using the sub-micron SiC powder as a raw material. When the growth temperature is at 1900 °C, the silicon carbide crystal is mainly 3C-SiC, with the growth temperature increased at 2100 °C, the characteristic diffraction peaks of the sample is 3C-SiC and 6H-SiC. The phase can be identified as pure α -SiC (6H) above 2200 °C. The peaks at $2\theta = 35.6^\circ$ and 75.4° , corresponding to the 6H-SiC (0 0 0 6) and (0 0 0 12) planes were observed in all the samples. Additionally, with an increasing temperature, the relative intensities of the peaks corresponding to the (0 0 0 1) planes significantly increased from 9000 to 28000, whereas the relative intensities of the other peaks gradually weakened.

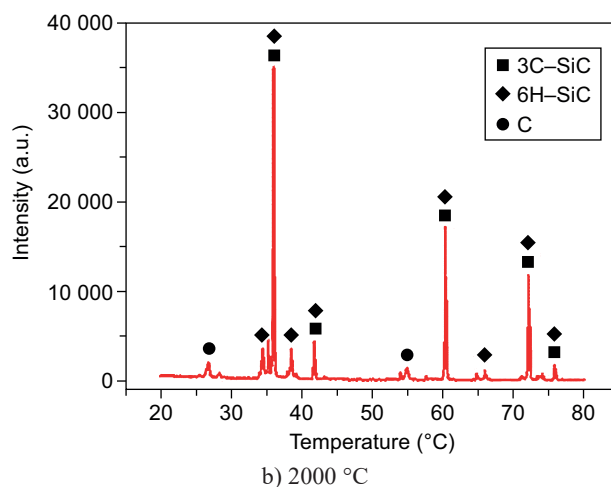
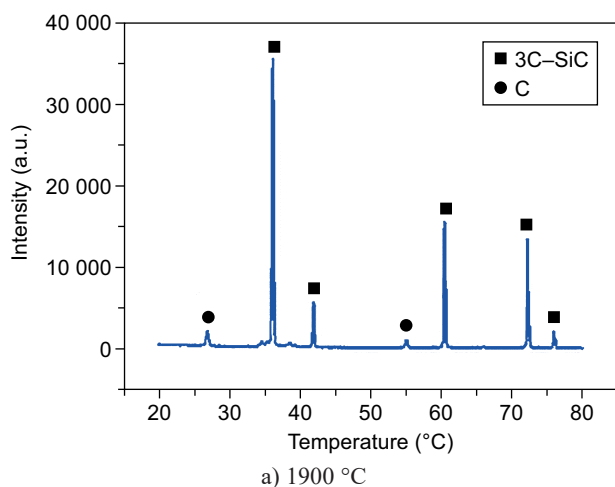


Figure 7. The XRD patterns of the SiC ceramic at the different sintering temperatures using the sub-micrometre-SiC powder as a raw material: a) 1900 °C, b) 2000 °C. (Continue on next page)

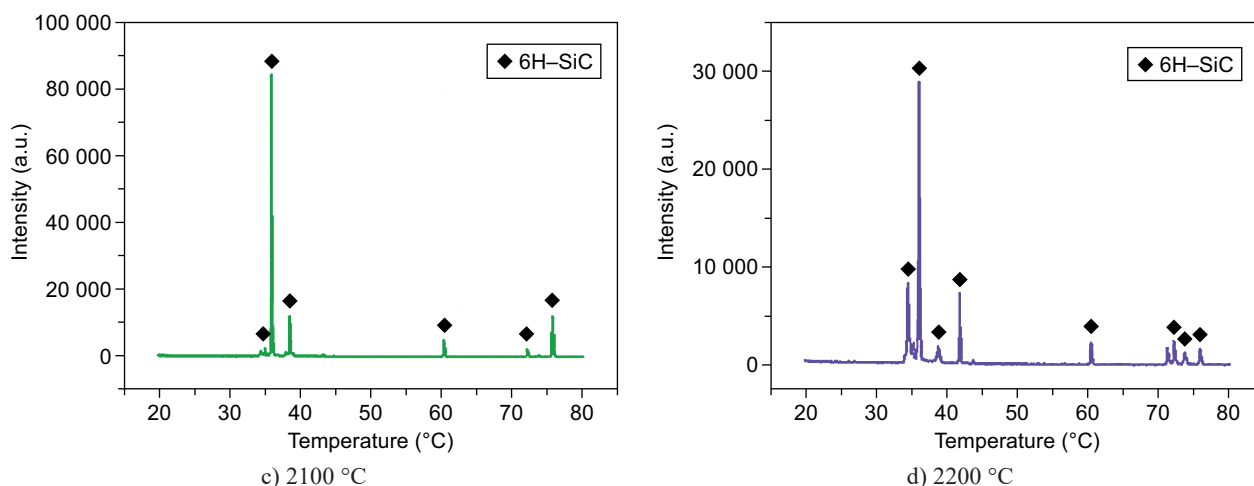
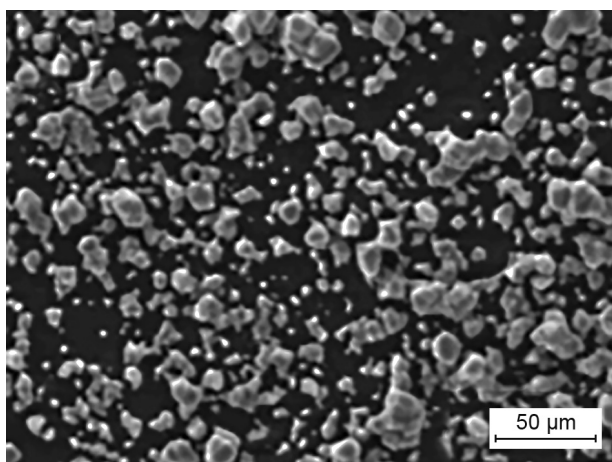


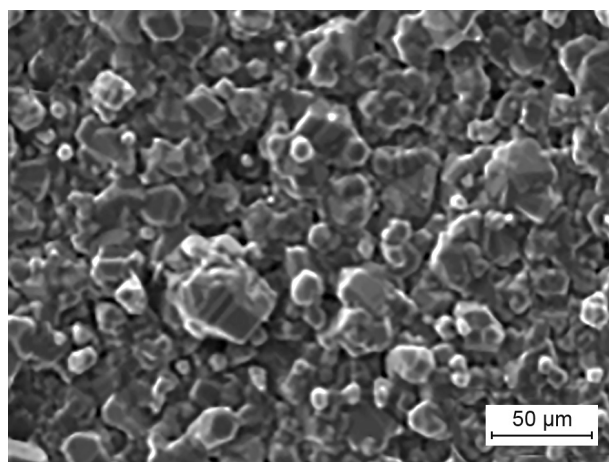
Figure 7. The XRD patterns of the SiC ceramic at the different sintering temperatures using the sub-micrometre-SiC powder as a raw material: c) 2100 °C, d) 2200 °C).

Figure 8 shows the SEM of the SiC grains obtained using the 500 nm powders grown at the different temperatures (1900 °C, 2000 °C, 2100 °C, 2200 °C) for 2 min. It can be seen that the number of the SiC grain size is relatively small in the samples grown at 1900 °C and the graphite substrates can also be seen. With the growth temperature increasing, the size of the grains increases gradually, and the graphite substrates disappear. It can be found that the morphology of the silicon carbide grains has developed to be hexagonal over 2100 °C, the regular columnar silicon carbide grains with the typical characteristics of α -SiC grains can be clearly seen. Because the nucleation rate of the silicon carbide raw material is higher and the growth rate is lower at lower temperatures, thus the number of grains observed is more and the size is smaller. With the increasing temperature, the nucleation rate decreases and the growth rate increases, so the number of grains observed decreases and the size increases.

Figure 9 show the SEM of the sample using the 500 nm powders growing at different times: 2 min; 8 min; 32 min; 60 min. It can be seen that the grain size is much smaller, and the large number of grains at 2200 °C for 2 min, the grains were arranged having a stacked manner existence and were relatively dense. With the holding time being increased, the grain size is relatively large, and the number of grains decreased, along with the growth of the grain orientation, the growth is about to begin, generating voids which appeared between the grains. When growth time is over 32 min, the crystal along the (0 0 0 1) surface orientation grows, the voids between the grains gradually increase, mainly due to the directional growth process, the other plane growth is slower, with the growth process of the crystal growth, the grain boundary diffusion gap between the grain boundaries decreases, and densified sintering at 60 min.

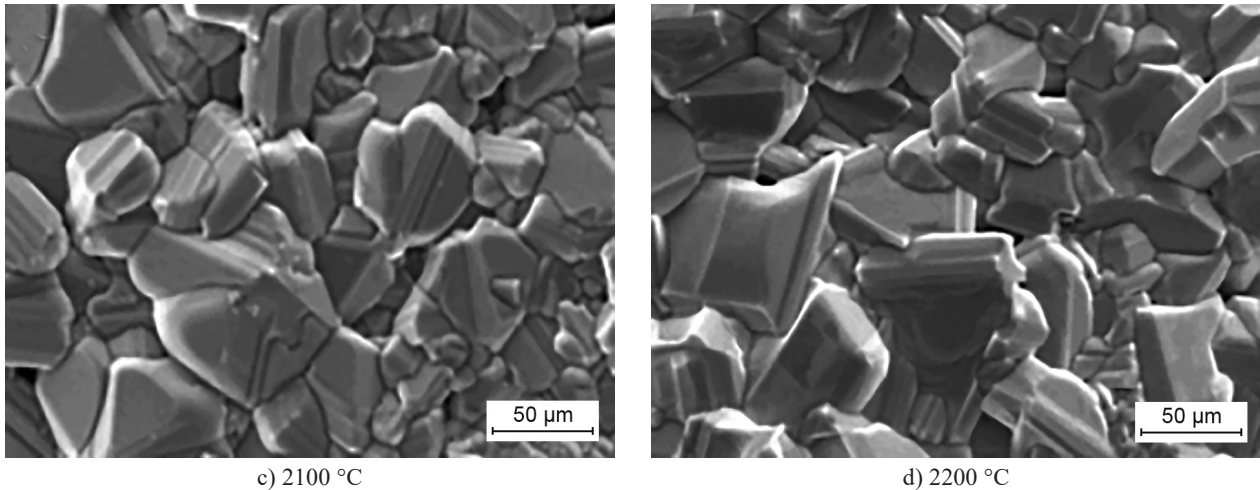


a) 1900 °C



b) 2000 °C

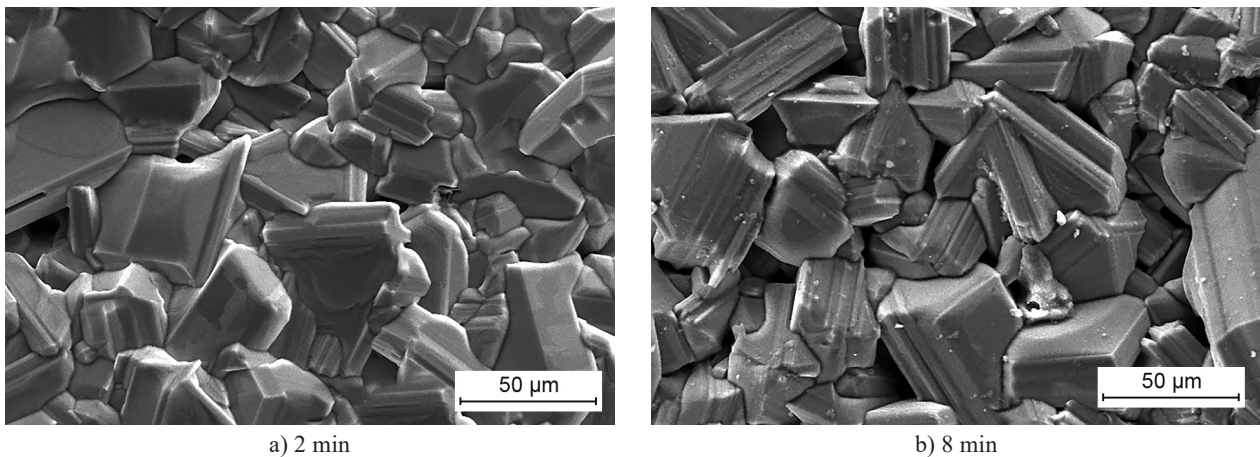
Figure 8. The SEM of the SiC grains growth obtained at the different temperatures: a) 1900 °C, b) 2000 °C. (Continue on next page)



c) 2100 °C

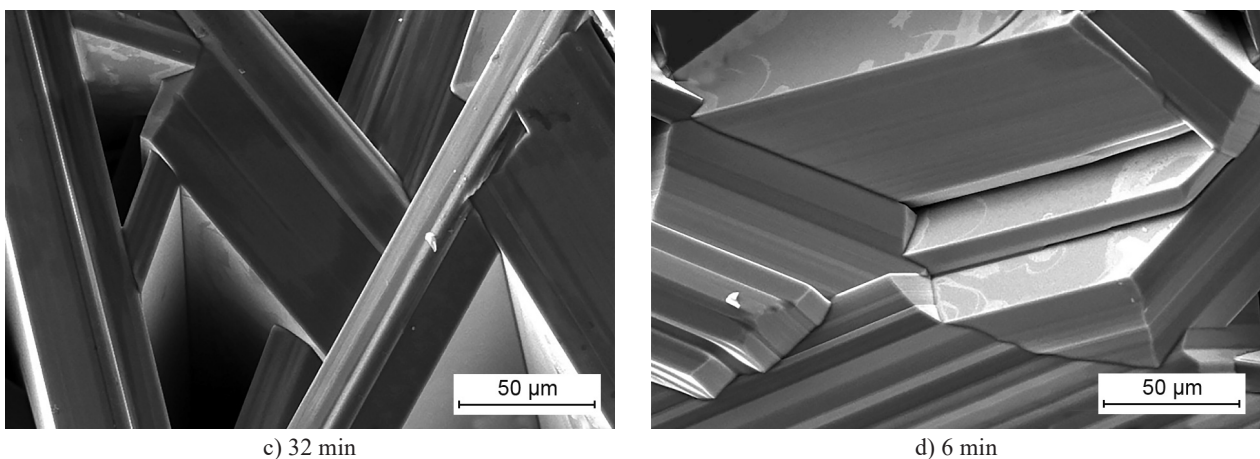
d) 2200 °C

Figure 8. The SEM of the SiC grains growth obtained at the different temperatures: c) 2100 °C, d) 2200 °C.



a) 2 min

b) 8 min



c) 32 min

d) 60 min

Figure 9. The SEM of the samples using 500 nm powders for the different growing time: a) 2 min; b) 8 min; c) 32 min; d) 60 min.

CONCLUSIONS

Dense SiC was prepared by a high-temperature physical vapour transport (PVT) method using sub-micron SiC powders (500 nm) as a raw material. The effects of the temperature and holding time on the grain size, growth rate, thickness and orientation of the silicon carbide were

explored, and the concentration gradient, random nuclei of the SiC on the polycrystalline phase growth during the SiC PVT growth were studied. The growth mechanism was explained from the thermodynamics and kinetics perspective. The result shows the grain size of the SiC nuclei increased with a growth temperature lower than 2200 °C, and decreased with a growth temperature higher

than 2200 °C. The XRD analysis shows the majority of the silicon carbide crystal β -SiC (3C-SiC) with a growth temperature lower at 2000 °C, and it is 6H-SiC above 2200 °C. From the 2000 to 2200 °C temperature range, the 3C-SiC decreases, but the 6H-SiC increases, while in this temperature range, the transition was from the 3C-SiC to the 6H-SiC phase. The microstructure shows that the growth of the silicon carbide has hexagonal columnar silicon carbide grains above 2200 °C, the average grain size of the SiC material is 100 μm , while the characteristics of the α -SiC grains is obvious. The silicon carbide ceramics exhibited a bending strength of only 335.6 MPa, a bulk density of 3.07 g·cm⁻³ and a Vickers hardness of 28.5 \pm 0.6 GPa.

Acknowledgments

This work was funded by the National Natural Science Foundation of China (NSFC, Grant No. 51672209), by the National Key R&D Program of China (Grant No. 2017YFB0310300), and the Natural Science Basic Research Plan in Shaanxi Province of China (Grant No. 2016JQ5046).

REFERENCES

- Lee S. K., Kim Y. C., Kim C. H. (1994): Microstructural development and mechanical properties of pressureless-sintered SiC with plate-like grains using Al₂O₃-Y₂O₃ additives. *Journal of Materials Science*, 29(20), 5321-5326. Doi: 10.1007/BF01171542
- Ravi B. G., Omotoye O. A., Srivatsan T. S., Petrorali M., Sudarshan, T. S. (2000): The microstructure and hardness of silicon carbide synthesized by plasma pressure compaction. *Journal of Alloys and Compounds*, 299(1-2), 292-296. Doi: 10.1016/S0925-8388(99)00815-4
- Fernández J. M., Muñoz A., de Arellano López A. R., Fera F. V., Dominguez-Rodriguez A., Singh M. (2003): Microstructure – mechanical properties correlation in siliconized silicon carbide ceramics. *Acta Materialia*, 51(11), 3259-3275. Doi: 10.1016/S1359-6454(03)00157-5
- Zhou T., Xu R., Ruan B., Liang Z., Wang X. (2018): Fabrication of microlens array on 6H-SiC mold by an integrated microcutting-etching process. *Precision Engineering*, 54, 314-320. Doi: 10.1016/j.precisioneng.2018.06.008
- Racka K., Tymicki E., Graszka K., Jakiela R., Pisarek M., Surma B., Avdonin A., Skupinski P., Krupka J. (2014): Growth of SiC by PVT method with different sources for doping by a cerium impurity, CeO₂ or CeSi₂. *Journal of Crystal Growth*, 401, 677-680. Doi: 10.1016/j.jcrysgro.2014.02.041
- Jun H. W., Lee H. W., Song H., Kim B. H., Ha J. (2004): Reaction-bonded silicon carbide tube fabricated by continuous sintering of double-walled preform. *Ceramics International*, 30(4), 533-537. Doi: 10.1016/j.ceramint.2003.09.022
- Zhang X. F., Yang Q., De Jonghe L. C. (2003): Microstructure development in hot-pressed silicon carbide: effects of aluminum, boron, and carbon additives. *Acta Materialia*, 51(13), 3849-3860. Doi: 10.1016/S1359-6454(03)00209-X
- Yuan R., Kruzic J. J., Zhang X. F., De Jonghe L. C., Ritchie R. O. (2003): Ambient to high-temperature fracture toughness and cyclic fatigue behavior in Al-containing silicon carbide ceramics. *Acta Materialia*, 51(20), 6477-6491. Doi: 10.1016/j.actamat.2003.08.038
- Jung E., Kim, Y., Kwon Y. J., Lee C. Y., Lee M. H., Lee W. J., ... & Jeong S. M. (2018): Synthesis of V-doped SiC powder for growth of semi-insulating SiC crystals. *Ceramics International*, 44(18), 22632-22637. Doi: 10.1016/j.ceramint.2018.09.039
- Racka K., Tymicki E., Graszka K., Kowalik I. A., Arvanitis D., Pisarek M., et al. (2013): Growth of SiC by PVT method in the presence of cerium dopant. *Journal of Crystal Growth*, 377, 88-95. Doi: 10.1016/j.jcrysgro.2013.05.011
- Gallardo-López A., Muñoz A., Martínez-Fernández J., Domínguez-Rodríguez A. (1999). High-temperature compressive creep of liquid phase sintered silicon carbide. *Acta Materialia*, 47(7), 2185-2195. Doi: 10.1016/S1359-6454(99)00072-5
- Guo X., Yang H., Zhang L., Zhu X. (2010): Sintering behavior, microstructure and mechanical properties of silicon carbide ceramics containing different nano-TiN additive. *Ceramics International*, 36(1), 161-165. Doi: 10.1016/j.ceramint.2009.07.013
- Cupid D. M., Fabrichnaya O., Seifert H. J. (2007): Thermodynamic aspects of liquid phase sintering of SiC using Al₂O₃ and Y₂O₃. *International Journal of Materials Research*, 98(10), 976-986. Doi: 10.3139/146.101557
- Kim Y. W., Lee S. H., Nishimura T., Mitomo M. (2005): Heat-resistant silicon carbide with aluminum nitride and scandium oxide. *Acta Materialia*, 53(17), 4701-4708. Doi: 10.1016/j.actamat.2005.07.002
- Shiramomo T., Gao B., Mercier F., Nishizawa S., Nakano S., Kakimoto K. (2014): Study of the effect of doped impurities on polytype stability during PVT growth of SiC using 2D nucleation theory. *Journal of Crystal Growth*, 385, 95-99. Doi: 10.1016/j.jcrysgro.2013.03.036
- Shiramomo T., Gao B., Mercier F., Nishizawa S., Nakano S., Kangawa Y., Kakimoto K. (2012): Thermodynamical analysis of polytype stability during PVT growth of SiC using 2D nucleation theory. *Journal of Crystal Growth*, 352(1), 177-180. Doi: 10.1016/j.jcrysgro.2012.01.023
- Dai P. Y., Wang Y. Z., Liu G. L., Wang B., Shi Y. G., Yang J. F., et al. (2011): Fabrication of highly dense pure SiC ceramics via the HTPVT method. *Acta Materialia*, 59(16), 6257-6263. Doi: 10.1016/j.actamat.2011.06.035
- Lilov S. K. (1995). Thermodynamic analysis of phase transformations at the dissociative evaporation of silicon carbide polytypes. *Diamond and Related Materials*, 4(12), 1331-1334. Doi: 10.1016/0925-9635(95)00312-6
- Shi Y., Yang J., Liu H., Dai P., Liu B., Jin Z., et al. (2012): Fabrication and mechanism of 6H-type silicon carbide whiskers by physical vapor transport technique. *Journal of Crystal Growth*, 349(1), 68-74. Doi: 10.1016/j.jcrysgro.2012.03.055
- Lin L., Zhu L., Zhao R., Tao H., Huang J., Zhang Z. (2019): Ferromagnetism induced by vacancies in (N, Al)-codoped 6H-SiC. *Solid State Communications*, 288, 28-32. Doi: 10.1016/j.ssc.2018.11.009

21. Van Rijswijk W., Shanefield D. J. (1990): Effects of carbon as a sintering aid in silicon carbide. *Journal of the American Ceramic Society*, 73(1), 148-149. Doi: 10.1111/j.1151-2916.1990.tb05109.x
 22. Lilov S. K. (1993): Study of the equilibrium processes in the gas phase during silicon carbide sublimation. *Materials Science and Engineering: B*, 21(1), 65-69. Doi: 10.1016/0921-5107(93)90267-Q
 23. Shi Y., Dai P., Yang J., Jin Z., Cheng J., Liu H. (2012): Effects of Grain Size of Source Material on Growing 6H-SiC Bulk Crystal by Physical Vapor Transport. *Materials and Manufacturing Processes*, 27(1), 84-87. Doi: 10.1080/10426914.2010.544829
-